4-2023

Vibration control of a two-story base-isolated building using a new tuned mass multi-sliding friction damper

Mohsen Amjadian
The University of Texas Rio Grande Valley, mohsen.amjadian@utrgv.edu

Syed Muhammad Bilal Haider
The University of Texas Rio Grande Valley

Vibration Control of a Two-Story Base-Isolated Building using a New Tuned Mass Multi-Sliding Friction Damper

Mohsen Amjadian[*a], Syed Muhammad Bilal Haider [a]
[a] Department of Civil Engineering, The University of Texas Rio Grande Valley, Edinburg, TX, USA 78539

ABSTRACT

This paper studies the use of a new Tuned Mass Multi-Sliding Friction Damper (TMMSFD) to increase the damping capacity of seismic isolators installed on a two-story base-isolated building to limit their lateral deformations. The proposed TMMSFD consists of a set of several masses that are laterally attached to the superstructure floor through linear springs. These masses are placed on top of each other one by one and are allowed to slide with respect to each other during the earthquake. The bottom mass that carries the weight of upper masses is in contact with the superstructure floor. The damping of system is supplied by the friction generated along the sliding friction surfaces. The TMMSFD has a low cost of installation, operation, and maintenance compared to common TMDs that use viscous fluid dampers for energy dissipation. The mechanical model of TMMSFD is installed on the numerical model of a two-story base-isolated building equipped with elastomeric rubber bearings in order to evaluate its performance in limiting the displacement of base floor. These models are created by the OpenSEESPy package which is a Python 3 interpreter of OpenSEES. A parametric study is performed to obtain the optimum design parameters of the TMMSFD including its total mass, frequency, and static friction coefficients of the siding surfaces for energy dissipation. The results of time-history analysis of numerical model show that the TMMSFD is capable of limiting the displacement of base floor with a little amount of friction implying its potential as a cost-effective tool for seismic protection.

Keywords: Vibration control, Tuned mass damper, Friction, Energy dissipation, and Seismic isolation.

1. INTRODUCTION

In recent years, significant progress has been made in improving the functional capabilities of civil structures and protecting it against the natural disasters like powerful earthquakes and strong winds. The idea of structural control systems has indeed made great strides in civil engineering. Different types of control systems, including active, passive, semi-active, and hybrid, are commonly employed. For instance, passive control systems have been put into practice in various high-rise building structures [1]. Of all the passive control techniques available, the tuned mass damper (TMD) stands out as one of the most effective and reliable control mechanism [2].

A tuned mass damper (TMD) is a type of passive control system that, in its most basic form, is composed of a mass, a spring, and a damping element attached to a structure to mitigate its dynamic response [3]. In the past, viscous dampers were widely utilized as the damping component in TMDs and have received extensive research and examination by many researchers. Viscous TMDs have been employed in a wide range of vibration control applications, including observatory towers, tall buildings, and other structures. Although, they are simple and efficient, however, viscous TMDs have some limitations too. Viscous TMDs dissipate energy through the viscous fluid in the damper, which can result in a large amount of heat being generated. This heat can cause the fluid to lose its viscosity, reducing the damping effect over time. They require regular maintenance to ensure that the fluid remains at the correct viscosity and that the damper is functioning properly. This can be time-consuming and expensive. Such TMDs are typically larger and heavier than other types of TMDs, making them less practical for use in small or lightweight structures. The dynamic stiffness of a viscous TMD is dependent on the viscosity of the fluid, which can change over time. This can result in a change in the damping behavior of the damper. Frictional TMDs (FTMDs) are often used to control vibrations in tall buildings, bridges, and other structures

[*] mohsen.amjadian@utrgv.edu; phone (956)665-5880; https://www.insdslab.com/.

that are susceptible to seismic or wind-induced vibrations. Due to their dependable solid-based energy dissipation mechanism, FTMDs have been demonstrated to be highly effective in dissipating seismic energy input in civil structures. Moreover, their low installation and operation costs, as well as their long-term durability, make them easy to manage. FTMDs have some advantages over other types of TMDs, such as viscous TMDs [4]. For example, FTMDs do not require any fluid or other consumable material, making them less prone to maintenance problems. They are also typically smaller and lighter than viscous TMDs, making them more practical for use in certain applications.

There have been several research studies conducted on FTMDs over the years. These studies have focused on various aspects of FTMDs, including their design, performance, and effectiveness in controlling vibrations in structures. Despite extensive studies on the design and implementation of traditional linear TMDs, the evaluation of nonlinear FTMDs for controlling the response of structures during earthquakes continues to be a subject of ongoing research interest. Etedali et al. examined how soil-structure interaction impacts the efficiency of TMDs and FTMDs in minimizing vibrations in tall buildings during near-field earthquakes [5]. Their results demonstrated that FTMDs are effective in reducing the peak kinetic and strain energies of the main structure, thus affirming that FTMDs are more capable of mitigating seismic energy and minimizing damage to tall buildings during near-field earthquakes compared to TMDs. Carmona et al. constructed a TMD that utilizes friction as its damping mechanism [6]. The TMD was implemented on a dynamic platform with low natural frequencies, which experienced excessive vibrations induced by human walking. To alleviate the amplitude vibrations produced when the platform is stimulated by human activities like walking or jumping, a passive control device was suggested that could be utilized in commercial buildings to decrease excessive vibrations caused by rhythmic human activities. Ricciardelli and Vickery investigated a single degree of freedom (SDOF) system with a tuned mass damper (TMD) that had linear stiffness and dry friction damping [7]. They also established guidelines for the design of friction TMD systems when evaluated under harmonic excitation. Salimi et al. sought to assess the benefits of the optimal design of friction TMD over conventional TMD for tall structures [8]. They evaluated the seismic performance of a 40-storey tall building and compared the results in terms of structural responses and energy. Gewei and Basu, in contrast, analyzed the dynamic properties of an SDOF system with an FTMD, using both harmonic and static linearization methods [9]. In addition, Pisal and Jangid examined the seismic response of a multi-story building equipped with multiple tuned mass friction dampers and evaluated the performance of FTMDs based on key factors such as mass ratio, tuning frequency ratio, and slip force [10].

In this study, a new FTMD with multi-sliding friction surfaces is proposed to increase the damping capacity of a two-story base-isolated building, reducing the lateral deformation of its isolation system. This passive control system is termed as Tuned Mass Multi-Sliding Friction Damper (TMMSFD) consisting of several masses attached to the superstructure floor with linear springs. These masses are arranged vertically and are allowed to slide with respect to each other during an earthquake, generating the friction that provides damping to the system. The bottom mass supports the weight of the upper masses and is in contact with the superstructure floor. The objective of this paper is to study how the multi-sliding friction surfaces enhance the energy dissipation capability of a FTMD and its effects on the seismic performance of primary structure overall.

2. DYNAMIC MODEL

2.1. Configuration of the proposed TMMSFD

Figure 1(a) shows the 3DOF dynamic model of a two-story base-isolated building with elastomeric rubber bearings and equipped with a typical FTMD installed on the roof of superstructure under an earthquake with the horizontal acceleration $\ddot{x}_g$. This model is designated as "Model 1" in which the displacement at the superstructure floor is denoted by x_s, the base floor by x_b, and the displacement of the FTMD by x_d all measured with respect to the ground. The displacement of FTMD with respect to the superstructure is defined as $u_d=x_d-x_s$. The normal force N_{f0} is constant and equal to the weight of FTMD as $N_{f0}=m_d g$ in this model. The friction force F_{f0} is generated when the mass slides on the surface of the superstructure floor. Figure 1(a) also indicates that m_b, m_s, and m_d are the mass of base floor, superstructure, and FTMD, respectively, whereas c_b, c_s, and c_d are the damping coefficients of base floor, superstructure, and FTMD, respectively. Lastly, k_b, k_s, and k_d shown in the figure describe are the stiffness coefficients of the base floor, superstructure, and FTMD, respectively. Model 1 has only one sliding friction surface.

Figure 1(b) shows a 4DOF dynamic model of the two-story base-isolated building equipped with the proposed TMMSFD that here it is assumed to have only two masses (n_d=2): the lower mass $m_{d1}=m_d/2$ and the upper mass $m_{d2}=m_d/2$ both installed on the superstructure floor. This model is designated as “Model 2”, which compared to Model 1 that has only one sliding friction surface, it has two sliding friction surfaces allowing the lower mass to slide over the surface of the superstructure floor with the constant normal force $N_{f1}=N_{f0}=(m_{d1}+m_{d2})g$ and the upper mass to slide over the top of the lower mass with the normal force $N_{f2}=N_{f0}/2=m_{d2}g$.

It should be noted that, in the proposed TMMSFD, the number of masses is not necessarily equal to 2 and can be increased ($n_d>2$). These masses are placed on top of each other one by one and are allowed to slide with respect to each other during the earthquake. Here, the bottom mass that carries the weight of upper masses is in contact with the superstructure floor.

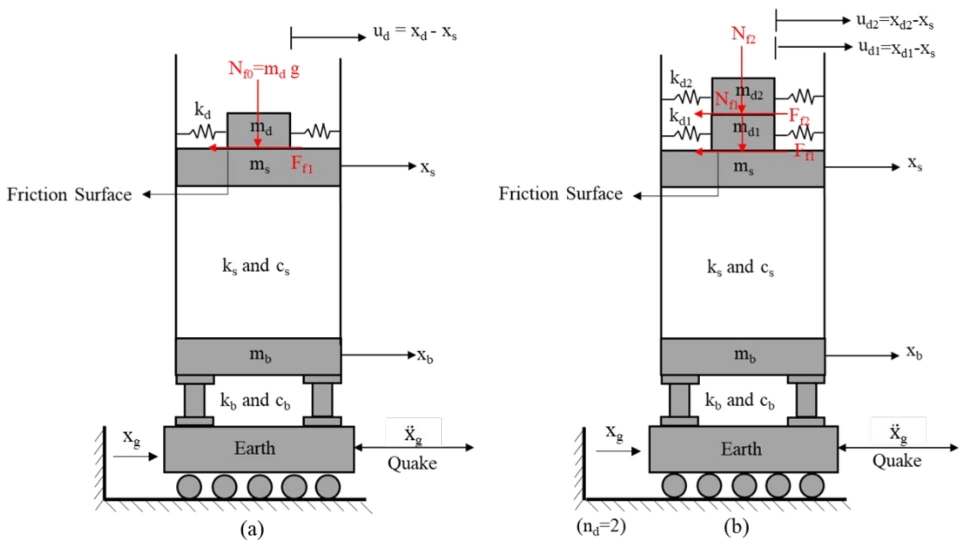

Figure 1. A FTMD mounted on the top floor of a base-isolated building subjected to horizontal ground motion with the (a) single sliding friction and (b) multi-sliding friction surfaces ($n_d=2$).

2.2. Equation of motion

The governing equation describing the motion of Model 2 in Figure 1(b) when subjected to an earthquake with the horizontal acceleration $\ddot{x}_g$ may be written into the following matrix form,

$$\mathbf{M\ddot{U}} + \mathbf{C\dot{U}} + \mathbf{KU} + \boldsymbol{\Lambda}_f\mathbf{F}_f = -\mathbf{M}\boldsymbol{\iota}_g\ddot{\mathbf{x}}_g \tag{1}$$

where $\mathbf{F}_f=\{F_{f1},F_{f2}\}^T$ is the friction force vector; $\mathbf{U} = \{x_b, x_s, x_{d1}, x_{d2}\}^T$ is the displacement vector; $\boldsymbol{\iota}_g = \{+1,+1,+1,+1\}^T$ is the ground acceleration influence vector; and $\boldsymbol{\Lambda}_f$, $\mathbf{M}$, $\mathbf{C}$, and $\mathbf{K}$ are the friction forces influence, mass, damping, and stiffness matrices which are defined as,

$$\mathbf{M} = \begin{bmatrix} m_b & 0 & 0 & 0 \\ 0 & m_s & 0 & 0 \\ 0 & 0 & m_{d1} & 0 \\ 0 & 0 & 0 & m_{d2} \end{bmatrix}, \mathbf{C} = \begin{bmatrix} c_b + c_s & -c_s & 0 & 0 \\ -c_s & +c_s & 0 & 0 \\ 0 & 0 & 0 & 0 \\ 0 & 0 & 0 & 0 \end{bmatrix}, \mathbf{K} = \begin{bmatrix} k_b + k_s & -k_s & 0 & 0 \\ -k_s & k_s + k_{d1} + k_{d2} & -k_{d1} & -k_{d2} \\ 0 & -k_{d1} & +k_{d1} & 0 \\ 0 & -k_{d2} & 0 & +k_{d2} \end{bmatrix}, \text{and } \boldsymbol{\Lambda}_f = \begin{bmatrix} 0 & 0 \\ -1 & 0 \\ +1 & -1 \\ 0 & +1 \end{bmatrix} \tag{2}$$

where m_b, m_s, $m_{d1}=m_d/2$, and $m_{d2}=m_d/2$ are the masses of base floor, the superstructure, the lower moving mass, and the upper moving mass, respectively; c_b and c_s are the damping coefficients of elastomeric rubber bearings in the base floor and the superstructure, respectively; and k_b, k_s, k_{d1}, and k_{d2} are the stiffness coefficients of elastomeric rubber bearings, the superstructure, and the springs attaching the lower and upper moving masses to the superstructure, respectively. The damping and stiffness coefficients of the elastomeric rubber bearings and the superstructure can be written as,

$$c_b = 2\xi_b(m_b + m_s)\omega_b, k_b = (m_b + m_s)\omega_b^2, c_s = 2\xi_s m_s \omega_s \text{ and } k_s = m_s\omega_s^2 \tag{3}$$

where ξ_b and ω_b are the critical damping ratio and natural frequency of the elastomeric rubber bearings, and ξ_s and ω_s are the critical damping ratio and natural frequency of superstructure. The friction forces F_{f1} and F_{f2} are described by the Coulomb friction model defined below [11], [12]:

$$F_{fi} = \mu_f N_{fi} \mathrm{sgn}(\dot{u}_{dfi}) \tag{4}$$

where μ_f is the coefficient of friction that is same for all the sliding friction surfaces (same friction materials), N_{fi} is the normal force acting on the i-th sliding friction surface with $N_{f1}=(m_{d1}+m_{d2})g$ and $N_{f2}=m_{d2}g$, and $\dot{u}_{dfi}$ is the sliding velocity of mass that for lower mass (i=1) is $\dot{u}_{df1} = \dot{u}_{d1}$ and for the upper mass is $\dot{u}_{df2} = \dot{u}_{d2} - \dot{u}_{d1}$. It is worth mentioning that the friction model described by Equation (3) does not take the stick-slip motion into account [13].

Table 1 shows the values of these parameters as recommended by Ramallo et al. (2002) for a smart base isolation system [4], [14].

Table 1. Key parameters of the base-isolated model shown in Figures 1(a) and (b) [4].

Parameter	Value	Unit
m_s	29485	kg
ω_s	20.944	rad/s
ξ_s	2	%
m_b	6800	kg
ω_b	2.513	rad/s
ξ_b	2	%

3. NUMERICAL MODEL

3.1. Finite element model

A two-dimensional finite element (2D FE) model of Model 2 is created by OpenSEESPy to solve the equation of motion described by Equation (1). Figure 2 shows the details on the FE model.

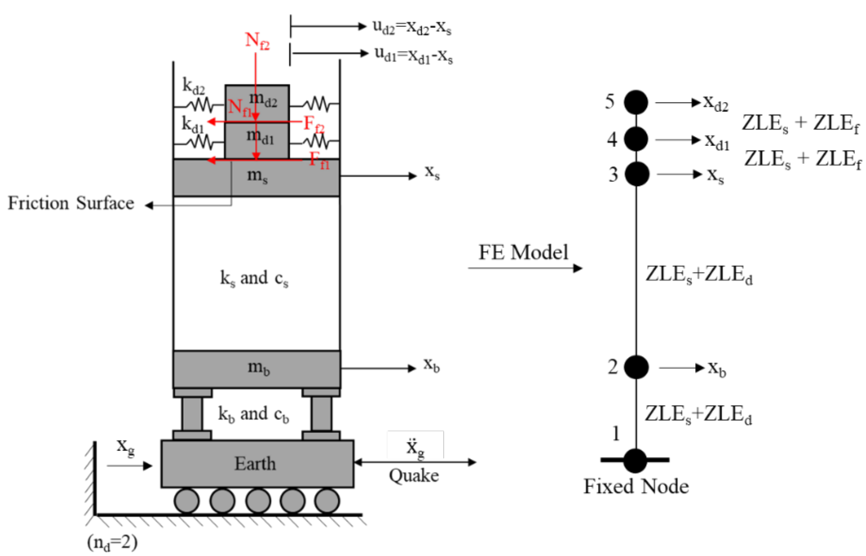

Figure 2. 2D FE model of Model 2 developed in OpenSEESPy.

As can be seen, the FE model consists of five nodes labeled from 1 to 5 representing the fixed support for the elastomeric rubber bearings, the base floor, the superstructure floor, and the lower and upper moving masses of the proposed TMMSFD, respectively. The masses m_b, m_s, m_{d1}, and m_{d2} are lumped at nodes 2 to 5, respectively, and while they are allowed to move freely in the x-direction, their motions are restrained in the y-direction.

The Zero-length element (ZLE) object in OpenSEESPy is used to model the developments of restoring and damping forces in the elastomeric rubber bearings and the superstructure, and the developments of the springs restoring forces and friction forces in the proposed TMMSFD. It should be noted that a ZLE object is defined by two nodes with the same coordinates. For this reasons, nodes 1 to 5 all are placed at same location but with different labels. In addition, the ZLE objects used to model the force-displacement behaviors of the linear springs (ZLE_s) and frictions (ZLE_f) in the proposed TMMSFD act in parallel.

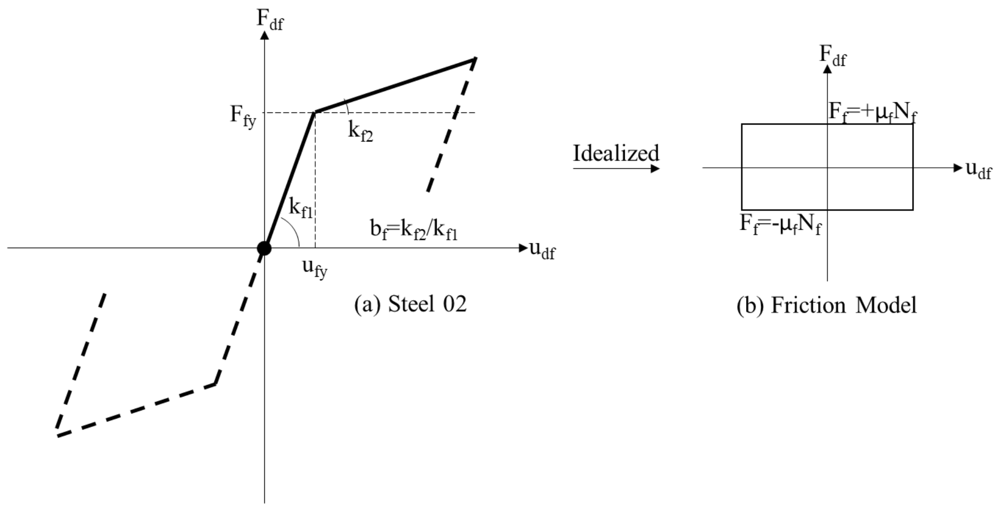

Figure 3. Modeling of the force-displacement behavior of friction developed on the sliding friction surfaces in OpenSEESPy: (a) Steel 02 Material (b) Coulomb friction model.

The force-displacement hysteresis loop of the Coulomb friction model has an ideal rectangular shape (See Figure 3(b)). The Steel02 material in OpenSEESPy with isotropic strain hardening is used to create this rectangular shaped hysteresis loop. Figure 3(a) shows the typical force-displacement curve generated by Steel02 material and its key parameters which are: u_{fy}=yielding displacement, F_{fy}=yield strength, and b_f=strain-hardening ratio that is defined as the ratio of post-yield stiffness ($k_{f2}=b_f k_{f1}$) to the initial elastic stiffness ($k_{f1}=F_{fy}/u_{fy}$). In this study, it is assumed that: u_{fy}=0.01 mm, $F_{fy}=\mu_f N_f$, and $b=10^{-9}$ to idealize the rectangular shape of the hysteresis loop of friction force in terms of displacement.

Table 2. Ground motion acceleration record used for the response history analysis [4].

RSN	Name	Year	Magnitude (M)	Station	Component	PGA (g)	PGA (g)
0169	Imperial Valley	1979	6.5	Delta	DLT352	0.350	0.384

3.2. Ground Motion Record

To study the time history response of a base-isolated building model, a far-field ground motion acceleration record from the PEER database is selected [4]. Table 2 shows the main properties of this record. The wavelet adjustment method, proposed by Hancock et al. (2006) [15], is utilized to modify and scale this record, so it matches the ASCE 7-10 Maximum Considered Earthquake (MCE) design response spectrum. The MCE represents an earthquake with a return period of approximately 2475 years, and it characterizes the seismicity of an area located in California with site class B, critical damping ratio of 5%, and PGA of 0.876g. The matching process is performed for the period range of T_n=0.5-5 s, as illustrated in Figure 4 (taken from [4]). This period range properly covers the period range of $0.5T_D$ to $1.25T_M$ recommended by ASCE 7-10. Here, T_D and T_M are the effective periods of the base-isolated building at the design and maximum displacements, respectively, where $T_D<T_b$ and $T_M<T_b$ with $T_b=2\pi/\omega_b$=2.5 s.

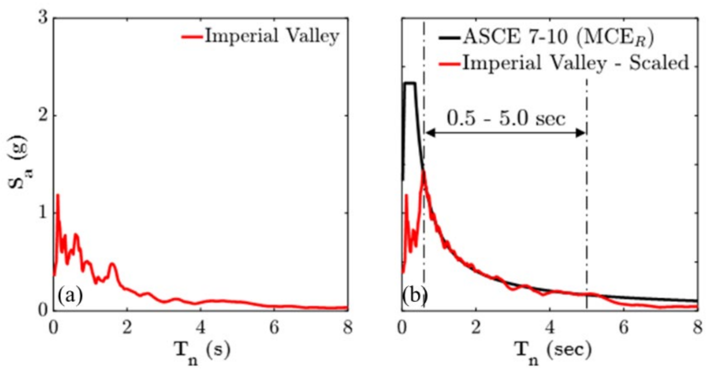

Figure 4. Acceleration design spectra of the ground motion record for 5%-damping (a) un-scaled (b) scaled to the ASCE 7-10 MCE design response spectrum for T_n=0.5 s to T_n=5.0 s [4].

4. RESULTS AND DISCUSSION

The key parameters of the proposed in addition to the number of mass used (n_d=2) are: (1) the mass ratio, μ_d=m_d/(m_d+m_s), (2) the frequency ratio, f_d=ω_d/ω_b, and (3) the coefficient of friction, μ_f.

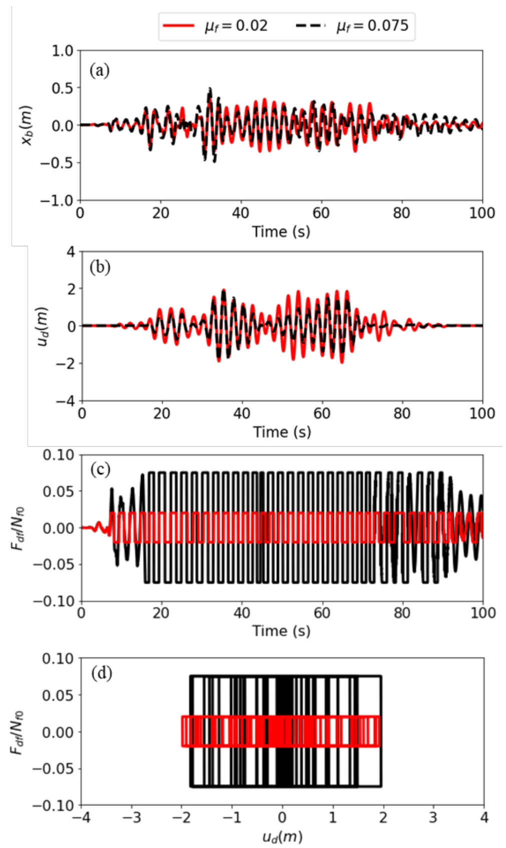

Figure 5. Comparison between the time history response of system for μ_f=0.02 and μ_f=0.075 in Model 1: (a) displacement of the base floor, (b) displacement of moving mass, (c) time history response of friction force, and (d) friction force-displacement hysteresis loop.

4.1. Time history analysis

In this section, first, we conduct a nonlinear time history response analysis on the two-story base-isolated building model equipped with a single sliding friction surface, i.e., Model 1 as shown in Figure 1. The parameters of the FTMD are assumed to be f_d=0.93, μ_d=0.050, and μ_f=0.02 (case 1). The results are compared to the case with f_d=0.93, μ_d=0.050, and μ_f=0.075 (case 2).

Figure 5(a) compares the time history displacement of the mass in case 1 with that in case 2. It is seen that the maximum displacement of the base floor in case 2 is equal to x_{bmax}=50 cm which is about 30% higher than that in case 1 that is about x_{bmax}=35 cm. This shows that although increasing the friction force in case 2 increases the energy dissipation capacity of the FTMD, it will not improve the seismic response of primary structure. The FTMD with lower friction force performs much better as it has a lower breakaway friction ($F_{fbr}=\mu_f N_{f0}$) that allows the mass to slide continuously during the ground motion, even when the intensity of ground motion is low. For example, see Figure 5(b) comparing the time history of displacement of the mass in case 1 to that in case 2. This figure shows the lack of slippage in the FTMD in case 2 when the intensity of ground motion is low which happens in the beginning (t<15 sec) and end (t>80 sec) of the earthquake. Figures 5(c) and (d) also compare the time history of the friction force and the force-displacement hysteresis loop of friction in these two cases, where the friction force has been normalized to the value of normal force N_{f0}.

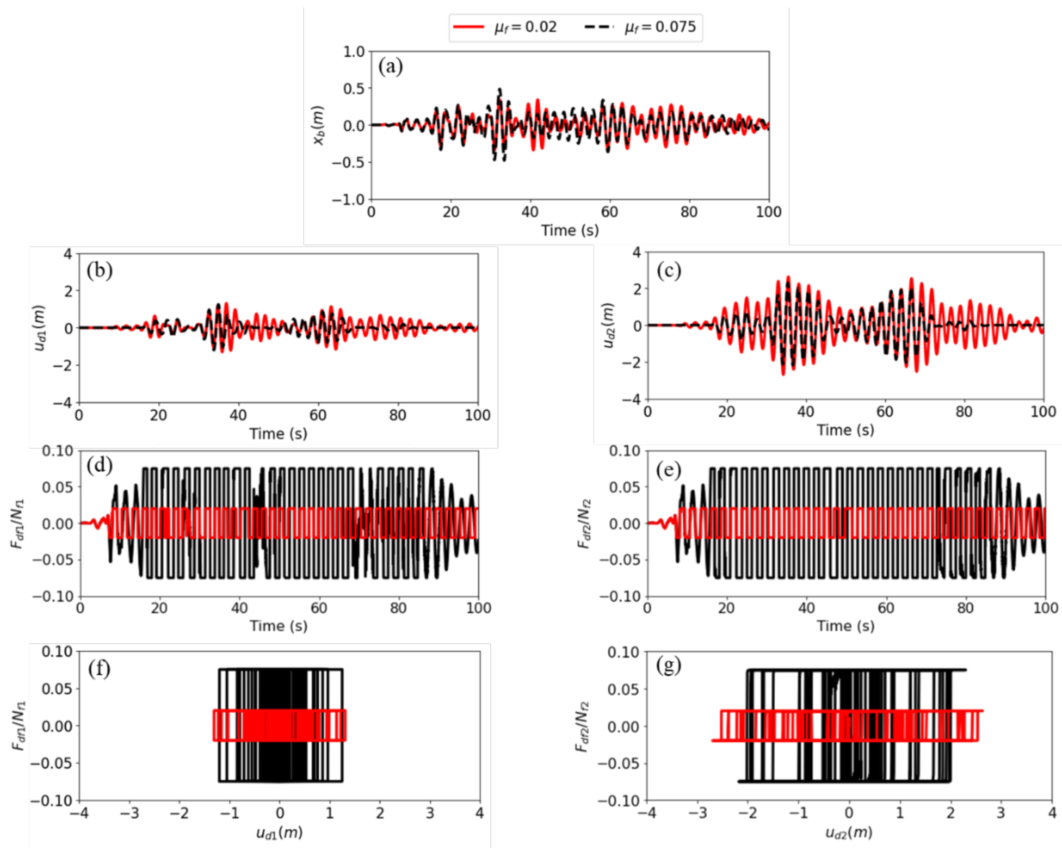

Figure 6. Comparison between the time history response of system for μ_f=0.02 and μ_f=0.075 in Model 2: (a) displacement of the base floor, (b),c displacement of the moving masses, (d,e) time history of friction forces, and (f,g) friction force-displacement hysteresis loops.

A nonlinear time history response analysis is carried out on the two-story base-isolated building model equipped with the proposed TMMSFD with two sliding friction surfaces, i.e., Model 2 as shown in Figure 1. The parameters of the FTMD are assumed to be f_{d1}=1.18, f_{d2}=0.93, μ_d=0.050, and μ_f=0.02 (case 1). The results are compared to the case with f_{d1}=1.18, f_{d2}=0.93, μ_d=0.050, and μ_f=0.075 (case 2).

Figure 6(a) shows the time history of displacement of base floor in case 1 to that in case 2. The maximum displacement of base floor in case 2 is higher than the corresponding value in case 1, as in the Model 1, this is due to the larger value of breakaway friction in case 2 implying the lack of a continuous slippage in the FTMD especially in the lower mass that has a higher breakaway friction force compared to that of the upper mass. This clearly can be observed in Figures 6(c) and

6(d) showing the time history displacements of the lower and upper masses. Figures 6(d) to 6(g) also compare the time histories of the friction forces and the force-displacement hysteresis loops of frictions developed on both the sliding friction surfaces in cases 1 and 2, where the friction forces have been normalized to the values of their corresponding normal forces, i.e., N_{f1} and N_{f2}.

4.2. Parametric study

In this section, a numerical searching approach is employed to optimize the parameters of FTMD systems in Model 1 and Model 2 shown in Figure 1. First, the performance of FTMD in Model 1 is evaluated in terms of the tuning frequency ratio and friction coefficient under the 1979 Imperial Valley earthquake. Figures 7(a-c) show the variation of maximum displacement of base floor versus the tuning frequency ratio and friction coefficient for μ_d=0.025, μ_d=0.050, and μ_d=0.075.

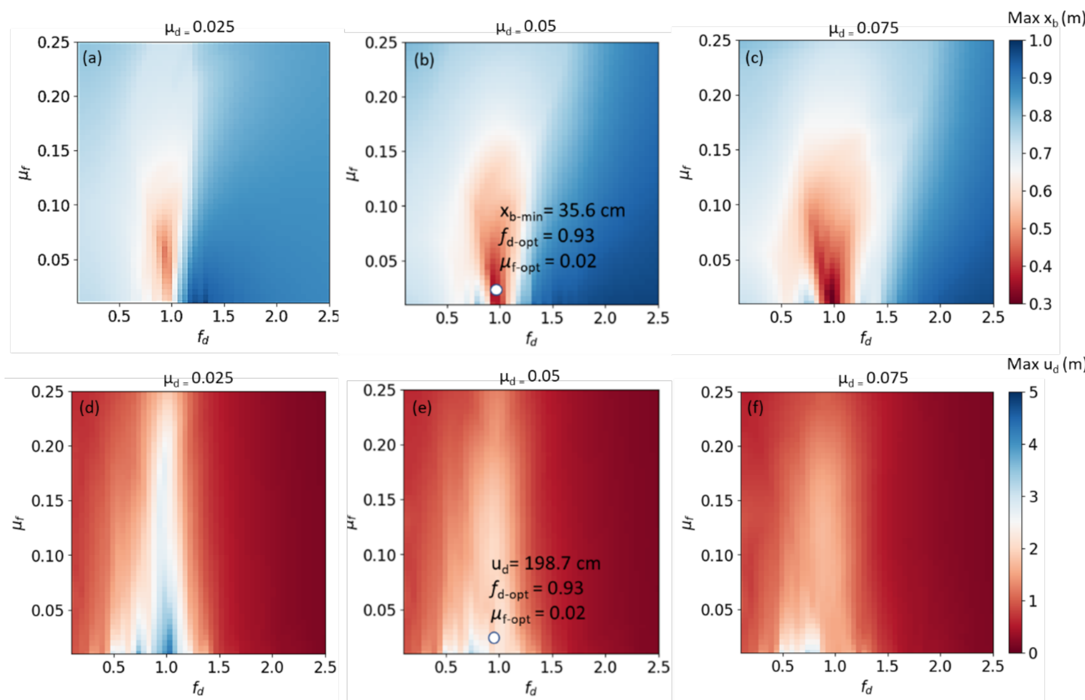

Figure 7. Variation of the maximum displacement of base floor (a-c) and the maximum displacement of the mass (d-f) with the tuning frequency and the friction coefficient in Model 1 for μ_d=0.025, 0.050, and 0.075.

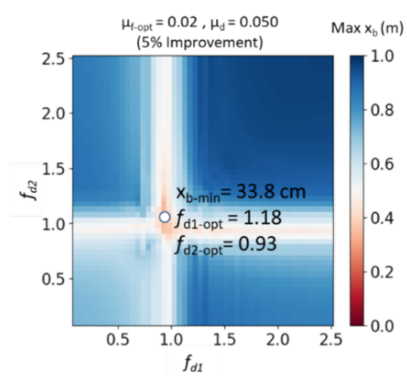

Figure 8. Variation of the maximum displacement of base floor with the tuning frequencies of lower and upper masses in Model 2 for μ_f=0.02 and μ_d=0.050.

This figure shows that the FTMD in Model 1 displays its best performance when it is approximately in resonance with the isolation system and the coefficient of friction is very low (μ_f<0.05). For larger values of friction coefficients, the risk of sticking increase in the FTMD as the breakaway friction increases that causes the FTMD to stop dissipating and storing the seismic input energy. The optimum parameters of the FTMD for μ_d=0.050 (m_d=1814 kg) are obtained as μ_f=0.02 and f_d=0.93, which results in a maximum displacement of base floor of x_{bmax}=35.6 cm. This shows 52.5% reduction in the base floor of base-isolated building under the 1979 Imperial Valley earthquake which is about x_{bmax}=75 cm. Figure 7(e) shows that the corresponding value for the maximum displacement of FTMD is about u_{dmax}=198.7 cm.

In the second part of this section, the performance of FTMD in Model 2, that represents the proposed TMMSFD, is evaluated in terms of the tuning frequency ratios of the lower and upper masses under the 1979 Imperial Valley earthquake. Here, it is, however, assumed that both the lower and upper sliding friction surfaces have a friction coefficient same as that in Model 1, i.e., μ_f=0.02. Figure 2 shows the variation of maximum displacement of base floor versus the tuning frequency ratios of the lower and upper masses for μ_d=0.050. It is seen that the FTMD in Model 2 displays its best performance when f_{d1}=0.93 and f_{d2}=1.18 which results in the maximum displacement of base floor x_{bmax}=33.8 cm indicating 5% improvement compared to FTMD in Model 1. This shows the superiority of proposed TMMSFD in which multi-sliding friction surfaces are used to reduce the breakaway friction force and lower the risk of sticking for the same amount of mass.

5. CONCLUSIONS

This paper investigates a novel TMMSFD that can enhance the damping capacity of a two-story base-isolated building, with the goal of minimizing the lateral deformation against earthquake. The proposed TMMSFD consists of two masses placed on each other and attached to the superstructure floor of primary structure through two linear springs while sliding relative to the primary structure through two sliding friction surfaces. It was shown that the proposed TMMSFD is capable of limiting the displacement of base floor with a little amount of friction implying its potential as a cost-effective tool for seismic protection. The primary result of this study shows that the proposed TMMSFD due to its multi-sliding friction surfaces feature is superior to a common type of FTMD with the same amount of mass as it has a lower breakaway friction and lower risk of sticking, especially, when the intensity of ground motion is low.

REFERENCES

[1] T. T. Soong and G. F. Dargush, Passive Energy Dissipation Systems in Structural Engineering. Wiley, 1997.

[2] G. C. Marano, R. Greco, F. Trentadue, and B. Chiaia, “Constrained reliability-based optimization of linear tuned mass dampers for seismic control,” Int. J. Solids Struct., vol. 44, no. 22–23, pp. 7370–7388, 2007.

[3] J. S. Love and T. C. Haskett, “The practical effects of friction for tuned mass dampers installed in tall buildings,” Eng. Struct., vol. 265, p. 114495, Aug. 2022, doi: 10.1016/j.engstruct.2022.114495.

[4] M. Amjadian, “A study on the use of an energy-regenerative tuned mass damper for vibration control and monitoring of base-isolated buildings,” in Active and Passive Smart Structures and Integrated Systems XVI, Apr. 2022, vol. 12043, pp. 252–261. doi: 10.1117/12.2610866.

[5] S. Etedali, M. Akbari, and M. Seifi, “MOCS-based optimum design of TMD and FTMD for tall buildings under near-field earthquakes including SSI effects,” Soil Dyn. Earthq. Eng., vol. 119, pp. 36–50, Apr. 2019, doi: 10.1016/j.soildyn.2018.12.027.

[6] J. E. C. Carmona, S. M. Avila, and G. Doz, “Proposal of a tuned mass damper with friction damping to control excessive floor vibrations,” Eng. Struct., vol. 148, pp. 81–100, Oct. 2017, doi: 10.1016/j.engstruct.2017.06.022.

[7] F. Ricciardelli and B. J. Vickery, “Tuned vibration absorbers with dry friction damping,” Earthq. Eng. Struct. Dyn., vol. 28, no. 7, pp. 707–723, 1999, doi: 10.1002/(SICI)1096-9845(199907)28:7<707::AID-EQE836>3.0.CO;2-C.

[8] M. Salimi, R. Kamgar, and H. Heidarzadeh, “An evaluation of the advantages of friction TMD over conventional TMD,” Innov. Infrastruct. Solut., vol. 6, no. 2, p. 95, Feb. 2021, doi: 10.1007/s41062-021-00473-5.

[9] Z. Gewei and B. Basu, “A study on friction-tuned mass damper: harmonic solution and statistical linearization,” J. Vib. Control, vol. 17, no. 5, pp. 721–731, 2011.

[10] A. Y. Pisal and R. S. Jangid, “Dynamic response of structure with tuned mass friction damper,” Int. J. Adv. Struct. Eng., vol. 8, no. 4, pp. 363–377, Dec. 2016, doi: 10.1007/s40091-016-0136-7.

[11] H. Olsson, K. J. Åström, C. Canudas De Wit, M. Gäfvert, and P. Lischinsky, “Friction Models and Friction Compensation,” Eur. J. Control, vol. 4, no. 3, pp. 176–195, Jan. 1998, doi: 10.1016/S0947-3580(98)70113-X.

[12] M. Amjadian and A. K. Agrawal, “A passive electromagnetic eddy current friction damper (PEMECFD): Theoretical and analytical modeling,” Struct. Control Health Monit., vol. 24, no. 10, p. e1978, Oct. 2017, doi: 10.1002/stc.1978.

[13] M. Amjadian, “Vibration Control using Frictional Tuned Mass Dampers with Stick-Slip Motion,” presented at the IMAC-XLI - Society for Experimental Mechanics, Austin, TX, 2023.
[14] J. C. Ramallo, E. A. Johnson, and B. F. Spencer, “‘Smart’ Base Isolation Systems,” J. Eng. Mech., vol. 128, no. 10, pp. 1088–1099, 2002, doi: 10.1061/(ASCE)0733-9399(2002)128:10(1088).
[15] J. Hancock et al., “An improved method of matching response spectra of recorded earthquake ground motion using wavelets,” J. Earthq. Eng., vol. 10, no. spec01, pp. 67–89, Jan. 2006, doi: 10.1142/S1363246906002736.